

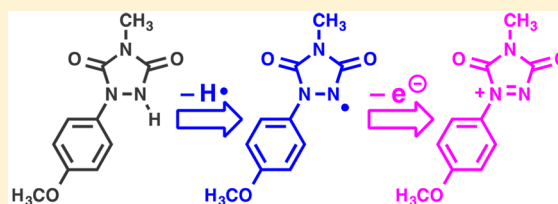
Intermediacy of a Persistent Urazole Radical and an Electrophilic Diazenium Species in the Acid-Catalyzed Reaction of MeTAD with Anisole

Gary W. Breton* and Alice H. Suroviec

Department of Chemistry, Berry College, Mount Berry, Georgia 30149, United States

S Supporting Information

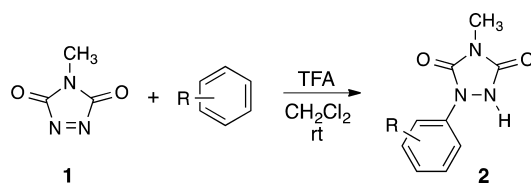
ABSTRACT: The reaction of *N*-methyl-1,2,4-triazoline-3,5-dione (MeTAD) with anisole in the presence of trifluoroacetic acid affords unexpected disubstituted urazole products instead of the expected monosubstituted urazole as typically observed in the reactions of MeTAD with other substituted benzenes. Our investigation into the mechanism of formation of these disubstituted products suggests that MeTAD is capable of further reaction with the initially formed monosubstituted urazole to afford a persistent urazole radical. The identity of this radical has been established by UV–vis spectroscopy, the nature of its self-dimerization reaction, and via independent generation. Electrochemical oxidation of this radical was carried out, and the resulting diazenium ion was demonstrated to be reactive with added substituted benzenes, including anisole. When oxidation was carried out chemically using thianthrenium perchlorate in the presence of anisole it was shown to produce the same disubstituted products (and in the same ratio) as observed in the acid-catalyzed reaction. A common diazenium species is proposed to be active in both cases. We also report the synthesis and characterization of three interesting tetrazane dimers resulting from unstable urazole radicals.



INTRODUCTION

We recently reported our studies on the trifluoroacetic acid (TFA) catalyzed reaction of *N*-methyl-1,2,4-triazoline-3,5-dione (MeTAD, **1**) with electron-rich aromatic rings to afford *N*-aryl urazoles (**2**) in good yields (Scheme 1).¹ This route provides for

Scheme 1. Reaction of MeTAD (1**) with Substituted Benzenes in the Presence of Trifluoroacetic Acid (TFA) To Afford Substituted Urazoles, **2****



the synthesis of substituted urazoles, compounds that have promising pharmaceutical applications, in a single synthetic step versus the three-step method that has traditionally been utilized.¹ While most of the aromatic compounds we studied behaved in a straightforward manner to afford the expected monosubstituted urazoles **2**, reaction of **1** with anisole afforded only small amounts of the monosubstituted urazole **3** (<6% yield, Scheme 2). Instead, the major products (44% yield) were the unexpected regioisomeric disubstituted urazole compounds **4a** and **4b** produced in an ~60:40 ratio, respectively. *N*-Methylurazole **5**, the reduced form of **1**, was also isolated in 40% yield. We suggested at the time that formation of disubstituted urazoles **4** could be rationalized if initially produced **3** was subject to further

oxidation to afford an electrophilic species such as diazenium intermediate **6** which could then react with anisole via a standard electrophilic aromatic substitution (EAS) process (Scheme 3).¹ In this work we present our studies on the mechanism of this reaction that led to some interesting observations and evidence for the intermediacy of a persistent urazole radical as well as the earlier-proposed diazenium electrophile.

RESULTS AND DISCUSSION

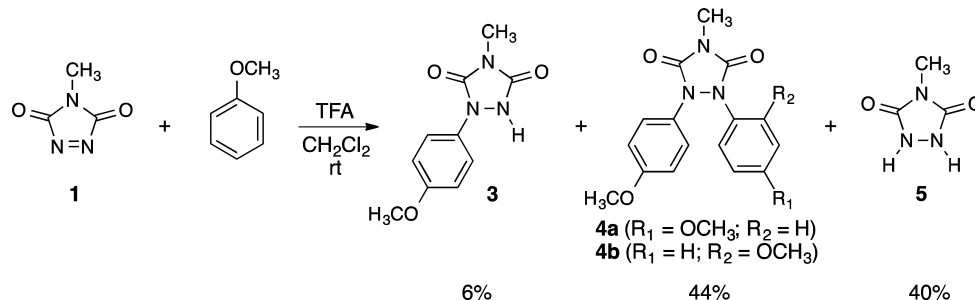
A. Involvement of a Persistent Urazole Radical. Control experiments confirmed that urazole **3** is unable to react on its own with anisole to afford compounds **4a,b** in the presence of TFA. Similarly, addition of MeTAD (**1**) alone to urazole **3** in the absence of acid catalyst did not afford disubstituted urazoles **4a,b**. However, almost immediately upon mixing of the characteristically red colored solution of **1** with colorless **3** in the absence of TFA, a deep purple colored solution resulted. Curious as to the source of this newly formed color, we mixed solutions of **1** and **3** in a quartz cuvette and observed the rapid formation of a new species by UV–vis spectroscopy (Figure 1A). Subtraction of the spectrum of **1** from that of the mixture revealed strong absorptions for this species at 345 and 629 nm and weaker absorptions at 423, 451, and 485 nm.

Several urazole radicals have previously been reported to be persistent (see Chart 1).² The 1- α -cumyl (**7**) and 1-*tert*-butylurazole (**8**) radicals are indefinitely persistent, while others,

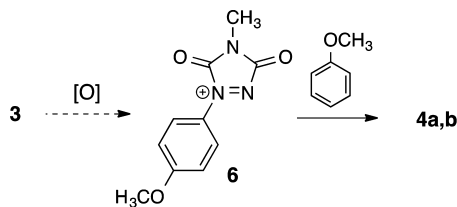
Received: November 2, 2015

Published: December 9, 2015

Scheme 2. Reaction of MeTAD (1) with Anisole To Afford Monosubstituted Urazole 3 and Disubstituted Urazoles 4a,b



Scheme 3. Possible Route for Formation of Disubstituted Urazoles 4a,b from Initially Formed Urazole 3 via a Proposed Intermediate Diazenium Species, 6



such as 1-phenylurazole (9), are transient, with 9 decomposing in solution within 24 h. Furthermore, the radicals have been reported to be in equilibrium with the corresponding tetrazane dimers (Scheme 4).^{2c} The tetrazane dimers of 7 and 8 can be isolated and purified as colorless solids. When these solids are dissolved in a solvent they provide deeply colored solutions of the corresponding free radicals. Pirkle reported that urazole radicals could be generated via treatment of the corresponding urazoles with oxidants such as *tert*-butyl hypochlorite, NBS, or (most cleanly) PbO₂.²

We found that treatment of urazole 3 with the commercially available heterogeneous oxidant Ni₂O₃ in CH₂Cl₂ followed by filtration afforded a deep blue solution of radical 10 (see Chart 1). The UV–vis spectrum of 10 was identical to that of the species generated via admixture of 3 and 1 as described earlier (Figure 1B). Radical 10 proved to be more persistent than 9, requiring nearly a week for complete loss of the blue color. The structure of 10 was further explored computationally at the UB3LYP/6-31G* level of theory (Figure 2A). The urazole ring remains coplanar with the aromatic ring which allows for delocalization of the unpaired electron not only within the urazole unit but also extending into the aromatic ring. Spin density is, therefore, observed not only on the two nitrogen atoms and adjacent carbonyl group oxygens of the urazole ring, as might be anticipated, but also at the *ortho* and *para* positions of the benzene ring as well as the oxygen atom of the OMe group (Figure 2B). Unlike unsubstituted urazole radical 9, however, which has been reported to decompose to an “uncharacterized precipitate”,^{2c} radical 10 undergoes clean dimerization to form compound 11 (Scheme 5). A proposed mechanism for the dimerization is provided in Scheme 5. Attack of one molecule of radical 10 onto a second is directed by bond formation between radical spin density on the nitrogen of one with the radical spin density at the *ortho* position of the benzene ring on the other. Hydrogen atom transfer from within the initial intermediate leads to the observed product, 11. When TFA was added to a solution of radical 10, dimerization to form 11 took place much more rapidly (within 45 min) in the presence of the acid catalyst

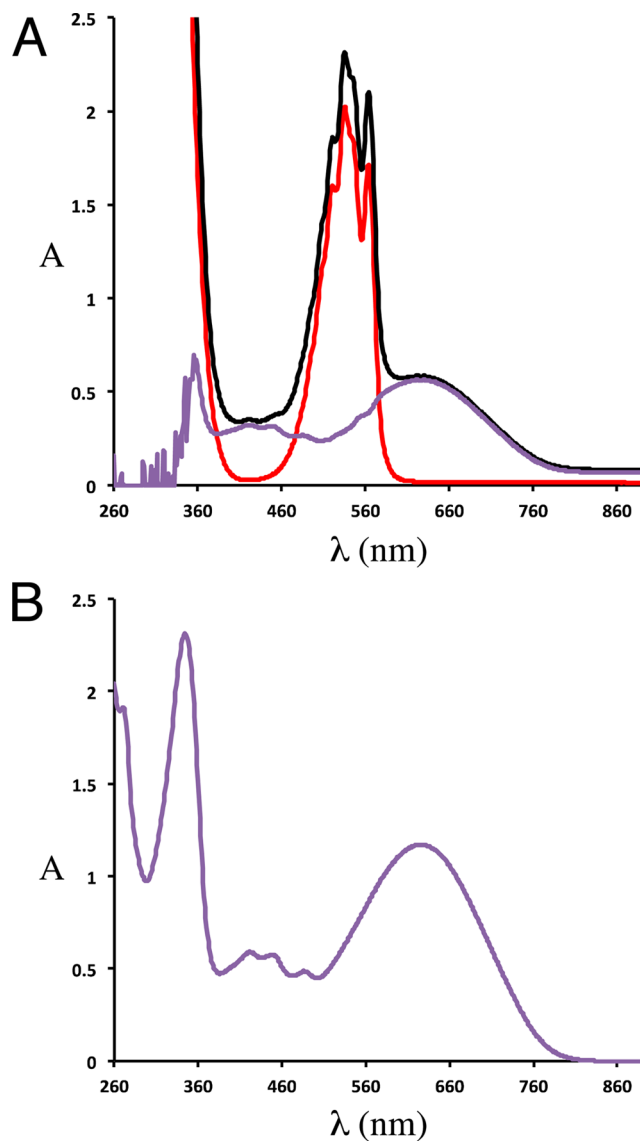
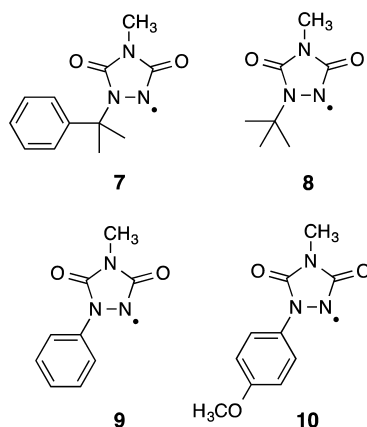


Figure 1. (A) UV–vis spectra of MeTAD (red) alone, a mixture of MeTAD and urazole 3 (black), and the result of subtracting the two spectra (purple). (B) UV–vis spectrum of independently generated urazole radical 10.

(a small amount of urazole 3 [6%] was also observed to form under these conditions). Finally, when a solution of 10 was allowed to react in the presence of an equivalent of urazole 3, uninterrupted dimerization of 10 to form 11 occurred over a period of 2 days and 3 was left untouched. The increase in the

Chart 1. Structures of Some Persistent Urazole Radicals



Scheme 4. Dimerization of Urazole Radicals To Form Tetrazane Dimers

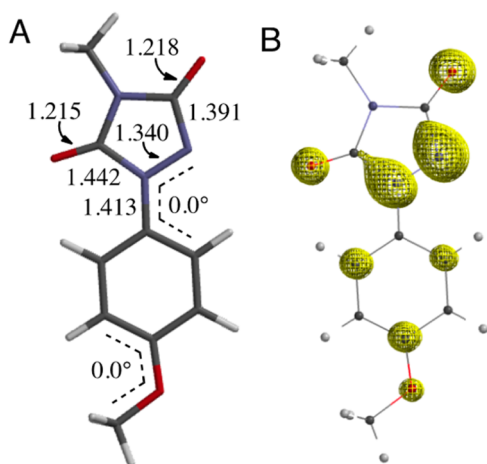
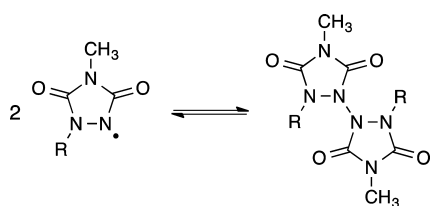
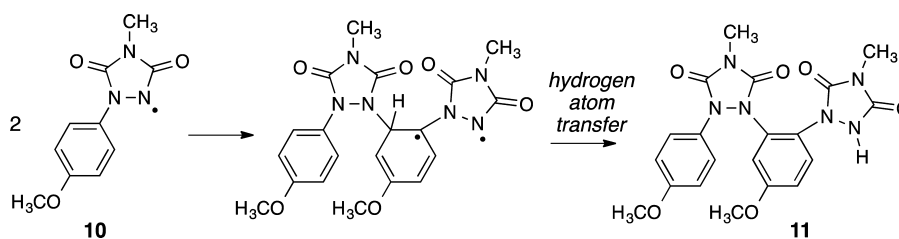
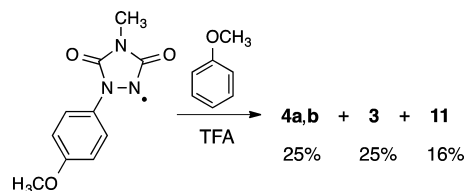


Figure 2. (A) Minimized structure of urazole radical **10** as calculated at the UB3LYP/6-31G* level of theory including some relevant bond distances (Å) and dihedral angles. (B) Resulting spin density map for urazole radical **10** (isovalue = 0.004).

rate of dimerization in the presence of **3** can be attributed to the ability of **3** to act as a weak acid catalyst ($pK_a = 4-5$).³

Scheme 5. Dimerization of Urazole Radical **10** To Form **11**

Mixing a solution of **10** with **1** in the presence of anisole did not produce any of the disubstituted products **4**. Thus, **1** alone is incapable of oxidizing urazole radical **10** in the absence of an acid catalyst. Interestingly, however, addition of trifluoroacetic acid to a solution of **10** alone in the presence of anisole resulted in the formation of a 60:40 mixture of **4a** and **4b** in 25% yield in addition to an equivalent amount of urazole **3** (Scheme 6). Dimer **11** was also formed in 16% yield. The significance of this experimental result with respect to the reaction mechanism will be revisited later.

Scheme 6. Acid-Catalyzed Reaction of Urazole Radical **10** in the Presence of Anisole To Form Disubstituted Products **4**

B. Evidence for the Intermediacy of a Diazenium Species. Electrochemical Generation of Diazenium **6**.

Knowing that radical **10** was readily generated by reaction of **1** with **3**, it seemed plausible that **10** might be subject to further oxidation to afford diazenium **6**, an electrophilic species which could be responsible for formation of the observed disubstituted compounds **4a,b** via a straightforward EAS reaction. To determine if generation of **6** from **3** was feasible, we conducted cyclic voltammetry experiments on acetonitrile solutions of **10** in the presence and absence of aromatic substrates. All experimental potentials are reported relative to SCE reference and at a scan rate of 50 mV/s unless otherwise specified.

Oxidation of **10** to diazenium **6** was observed to occur at $E_{p[ox]} = 1.17$ V followed by reduction back to the radical at $E_{p[red]} = 1.08$ V (O_1 and R_1 , respectively, in Figure 3A). The peak-to-peak separation ($E_{p[ox]} - E_{p[red]}$) was 90 mV at 50 mV/s but increased gradually as the scan rate was increased (to 140 mV at 1000 mV/s). Additionally, the ratio of the currents measured at the two electrochemical events, $I_{p[ox]}/I_{p[red]} = 1.42$, is greater than unity (i.e., the value consistent with a reversible process).⁴ Given these observations, we judge this process to be only partially reversible most likely because of the competing chemical reaction of the oxidized species (vide infra). When the cyclic voltammogram was conducted in the presence of anisole (5 equiv), although the oxidation event (O_1) was unaffected ($E_{p[ox]} = 1.14$ V in the presence of anisole), the reduction event was no longer observed (Figure 3B). This indicates that anisole is capable of trapping the generated diazenium species **6**, presumably via an EAS process. A similar result was observed in the presence of electron-rich mesitylene. Toluene is considerably less active

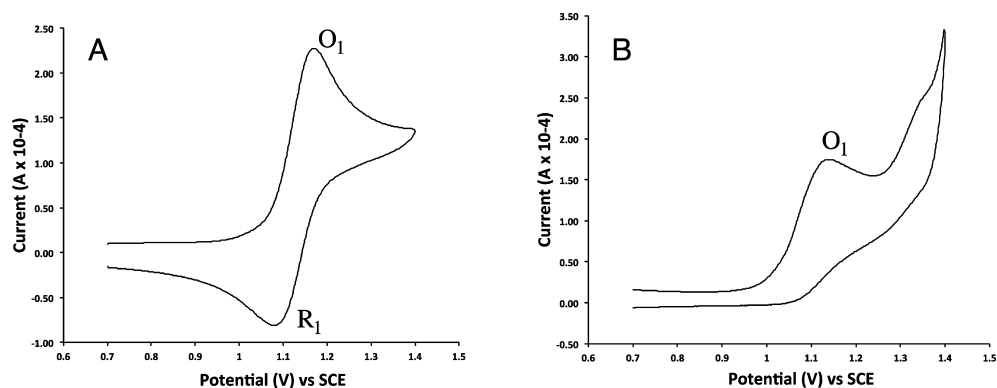


Figure 3. (A) Cyclic voltammogram (CV) of a solution of **10** (4.5 mM) in acetonitrile containing TBAF (0.1 M) as supporting electrolyte, starting at low potential (oxidative events are positive). (B) CV of a solution of **10** immediately after the addition of 5 equiv of anisole to the solution.

toward electrophilic aromatic substitution than either mesitylene or anisole.⁵ Hence, when the oxidation was conducted in the presence of toluene, both the reduction and oxidation events were unaffected ($I_{p[ox]}/I_{p[red]} = 1.49$) suggesting the generated diazenium species is not sufficiently electrophilic to react with toluene.

The parent urazole **3** was also subjected to analysis by cyclic voltammetry. Unlike radical **10**, urazole **3** has very limited solubility in acetonitrile and a saturated solution of unknown concentration was analyzed. A two-electron oxidation event at $E_{p[ox]} = 1.18$ V (i.e., essentially identical to the oxidation potential for **10**) was observed (O_1 in Figure 4), followed by an

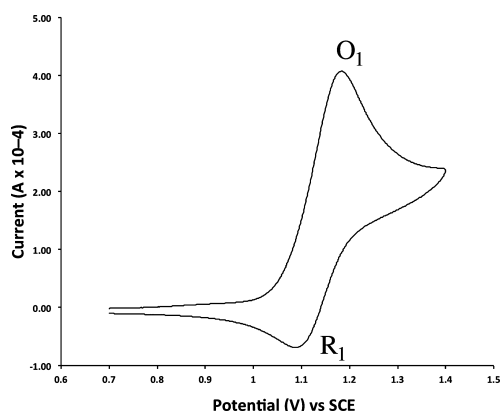


Figure 4. CV of urazole **3** in acetonitrile and TBAF (0.1M) as supporting electrolyte, starting at low potential (oxidative events are positive).

approximately one-electron reduction at $E_{p[red]} = 1.09$ V (R_1 in Figure 4) as suggested by $I_{p[ox]}/I_{p[red]} = 2.55$. Thus, a single electron oxidation of the urazole to form radical cation **12** appears to be rapidly followed by deprotonation to **10** which is already at an electrode potential sufficient to effect a second oxidation to **6** (see Scheme 7). Single electron reduction of the generated **6** to afford **10** then occurs uneventfully.

Interestingly, upon oxidation of **3**, a deep purple colored species, most likely that of **6**, was observed to coat the working electrode (Figure 5). Upon reduction, the color was lost. Presumably the same process occurs during formation of **6** from radical **10**, but the deep blue color of solutions of **10** prevents its observation. When the electrode potential was held just positive of that of $E_{p[ox]}$, a purple film appeared on the electrode, but then dissipated within a few seconds, and the reduction event was no

Scheme 7. Proposed Sequence of Electrochemical Events during CV Analysis of Urazole **3**

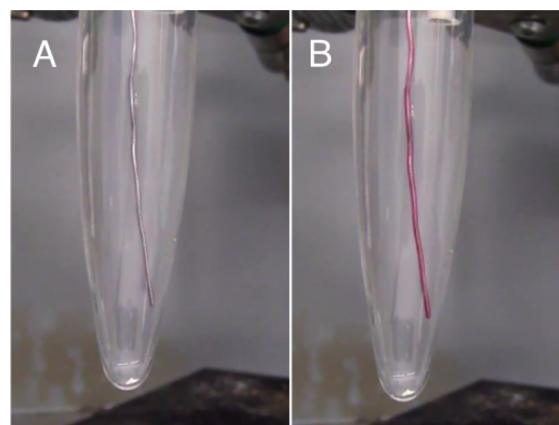
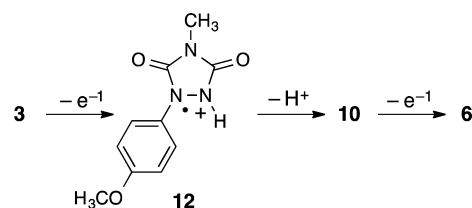
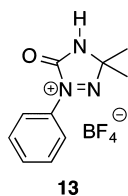


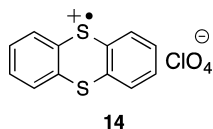
Figure 5. (A) Appearance of the platinum working electrode during collection of the CV of urazole **3** prior to the oxidation event (O_1 in Figure 4) as well as past the reduction event (R_1). (B) Electrode during the oxidation event.

longer observed. These observations suggest that diazenium **6** is not a stable species. When the cyclic voltammogram was conducted in the presence of anisole, while the oxidation remained unaffected, the reduction was no longer observed (as was the case for **10**) and there was no indication of color formation on the working electrode suggesting rapid quenching of generated **6**.

The instability of **6** is easily rationalized by the close proximity of the two electron-withdrawing carbonyl groups relative to the positively charged nitrogen atoms. The most closely related diazenium species we could find in the literature is that of **13**,⁶ which lacks the second carbonyl group adjacent to the azo group. Interestingly, diazenium **13** is reported to be isolable as the tetrafluoroborate salt. Unfortunately, however, neither its electrochemical properties nor its chemical reactivity has been described.



Chemical Generation of Diazenium 6. Given the apparent success of electrochemical generation of diazenium 6, we were keen to test whether we might be able to chemically oxidize radical 10 to diazenium 6 in solution. We selected thianthrenium perchlorate, 14, as a suitable one-electron oxidant because of its ready solubility in acetonitrile and the ease with which the reduced thianthrene form could be separated from our expected products.⁷



Our initial experiment involved dropwise addition of a solution of 14 to a preformed solution of 10 in the presence of anisole. We realized quite early, however, that addition of even a catalytic amount of oxidant was sufficient to deplete the deep blue color of 10 in just a few minutes. Disubstituted compounds 4a,b (60/40 ratio) were observed in a yield (32%) strikingly similar to that observed for the trifluoroacetic acid catalyzed reaction of 10 with anisole described earlier. Similarly, an equivalent amount of urazole 3 (29% yield) was also isolated. Evidently, small amounts of acid generated from the initial EAS process further catalyzed the reaction in a manner similar to that of TFA.

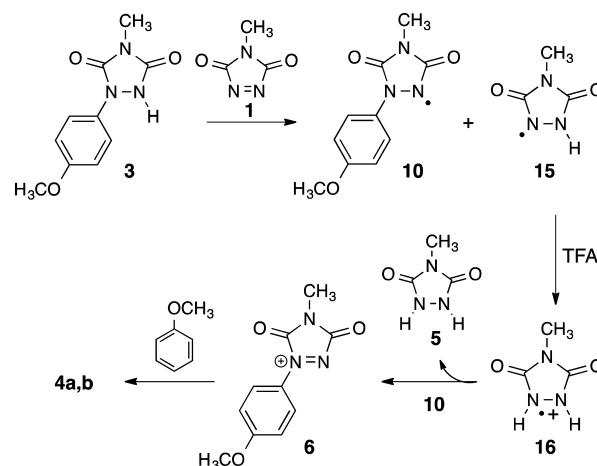
To prevent the acid-catalyzed reaction route we added an equivalent of the non-nucleophilic base 2,6-lutidine to act as a proton sponge. In the presence of 2,6-lutidine, under otherwise identical conditions, it required the dropwise addition of 0.72 equiv of 14 to deplete the deep blue color of 10, suggesting that the radical was effectively formed in 72% yield from Ni₂O₃ oxidation of the urazole. A mixture of compounds 4a,b was isolated from the reaction in a ratio of ~60:40 in 55% yield (or 76% yield based on 72% yield for the radical formation process). No other products were observed apart from that of the thianthrene byproduct. The observed ratio of products 4a,b was essentially identical to that observed from the direct reaction of MeTAD with anisole in the presence of TFA suggesting that the diazenium ion 6 is most likely an intermediate in both reactions. Furthermore, the same product ratio is observed from the acid-catalyzed reactions of 10 with anisole, implicating 6 as a common intermediate in all of these reactions.

In a separate experiment, a solution of 14 was added dropwise to a solution of 10 and 2,6-lutidine in the initial absence of anisole. Immediately upon consumption of the deep blue color of the radical (again requiring only 0.75 equiv of 14), anisole was immediately introduced into the stirring reaction mixture. Under these conditions, however, a complex reaction mixture was obtained, and there was no indication of formation of compounds 4a,b. This experiment confirmed what the cyclic voltammetry experiments had previously suggested, that diazenium 6 is an unstable species.

C. A Proposed Reaction Mechanism. As put forward in our previous work,¹ initial reaction of 1 with anisole in the presence of an acid catalyst to afford urazole 3 is expected to

proceed via a typical EAS reaction. The UV-vis experiments reported in this work have established that 1 is capable of further reaction with 3 via hydrogen atom abstraction to generate readily observable concentrations of radical 10 and presumably urazole radical 15 (Scheme 8).

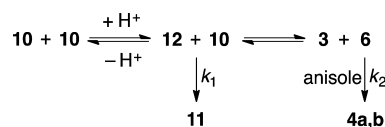
Scheme 8. Proposed Mechanism for the Formation of Disubstituted Urazoles 4a,b from Initially Formed Urazole 3 via Intermediate Diazenium 6



Protonation of 15 by TFA would afford radical cation 16 that is capable of oxidizing radical 10 to form intermediate diazenium 6. Cyclic voltammetry experiments demonstrated that oxidation of *N*-methylurazole (5) to form radical cation 16 occurs at higher oxidation potential ($E_p = 1.52$ V) than does oxidation of 10 ($E_p = 1.17$ V) rendering 16 a viable oxidant for 10.⁸ Thus, the formation of 5 as a byproduct from the reaction (40% yield) is accounted for by this mechanism as well as a nearly equivalent amount of disubstituted compounds 4a,b (44% yield) resulting from the subsequent reaction of 6 with anisole. Radical 10 could also potentially be oxidized to diazenium 6 by protonated 10 (i.e., 12) in addition to oxidation by 16. However, the low yields of urazole 3 (the expected byproduct of oxidation) derived from the acid-catalyzed reaction of MeTAD with anisole suggest this is a minor reaction route at best.

As described earlier, treatment of solutions of radical 10 with an acid catalyst (either TFA or acid byproduct from introduction of a catalytic amount of 14) in the presence of anisole produced 4a,b in the same 60:40 ratio as the MeTAD/TFA reaction suggesting the common intermediacy of diazenium 6. Under these circumstances it must be that protonated 10, i.e., 12, is acting as the oxidant for 10 to generate urazole 3 and diazenium 6, which then reacts with anisole to form 4a,b (see Scheme 9). This accounts for the formation of equivalent yields of 4a,b and 3 from the acid-catalyzed reactions. Additionally, only small amounts of dimer 11 were formed under these conditions, suggesting that trapping of diazenium 6 by anisole is a faster reaction than is acid-catalyzed formation of dimer 11 (i.e., $k_2 >$

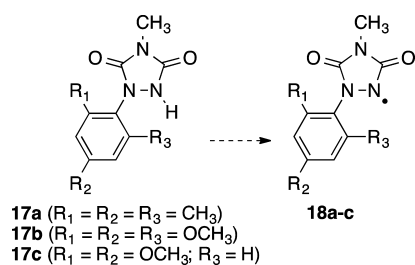
Scheme 9. Proposed Processes between Active Species in Solutions of 10 in the Presence of an Acid Catalyst



k_1). Recall, however, that when TFA *alone* was added to a solution of **10**, the predominant reaction route was dimerization to **11**, and only a minor amount of urazole **3** (6% yield) was obtained. Any diazenium **6** formed from oxidation of **10** by **12** in the absence of anisole does not react with the aromatic rings of either radical **10** or dimer **11**, most likely for steric reasons. Therefore, under these conditions, any **6** formed is most likely reduced back to **10** (by **3**) via an equilibrium process (Scheme 9). Consistent with these observations is the fact that acid-catalyzed consumption of **10** in the presence of anisole is considerably faster (3 min) than reaction in its absence (45 min).

Finally, we attempted to determine if **12** could act as an independent electrophile in its reaction with anisole. To this end, a solution of **10** was added dropwise over an hour to a solution of anisole and TFA in an attempt to keep the concentration of **10** (and therefore **12**) low in order to prevent oxidation of **10** by a molecule of **12**. The deep blue color of the radical was initially rapidly discharged with each drop of solution. As further addition occurred, however, while the blue color continued to be rapidly discharged, a pale emerald green color gradually developed which remained at reaction's end. Interestingly, we obtained results nearly identical to those of the reaction in which TFA was added directly to a mixture of **10** and anisole; i.e., a 35% yield of **4a,b** (60/40 ratio) and a 29% yield of **3** were isolated. Hence, **12** is apparently not capable of reacting with anisole alone via an EAS reaction or a yield of **4a,b** significantly greater than that of **3** would be expected.

Scheme 10. Urazole Radicals (**18a–c**) Potentially Formed via Hydrogen Abstraction from Urazoles **17a–c**



One question remains unanswered at this point: why were disubstituted products only observed in the acid-catalyzed reaction of **1** with anisole and not with the other substituted benzene substrates investigated in the original study (e.g., 1,3-

dimethoxybenzene, 1,3,5-trimethoxybenzene, mesitylene, etc.)?¹ A clue to this mystery is found in the earlier described UV–vis experiment in which **1** was mixed with urazole **3** to rapidly form appreciable concentrations of radical **10**. Interestingly, when **1** was similarly mixed with urazoles **17a–c** (i.e., the urazoles formed from EAS reaction of **1** with the aromatic substrates above), the UV–vis spectra remained unaffected and the production of new species, including the expected corresponding radicals **18a–c**, was not observed to occur (Scheme 10). One source of stability for radical **10** derives from its ability to maintain coplanarity of the urazole ring with the aromatic system that allows for extended delocalization of the unpaired electron as discussed earlier (Figure 2). We suspected that the *ortho*-substituents on the aromatic rings of **18a–c** might prevent similar coplanarity of the two ring systems and thereby lessen their stabilities. Thus, as for **10**, we minimized the structures of the radical species **18a–c** (see Figure 6) at the B3LYP/6-31G* level of theory. As expected, the urazole rings were incapable of attaining planarity with the benzene rings due to steric hindrance. The dihedral angles between the two rings were found to be 62.9° for **18a**, 69.9° for **18b**, and 44.7° for **18c**. Thus, the extent of delocalization of the unpaired spin, and expected commensurate stabilization, is attenuated relative to that of **10** (compare Figures 2 and 6).

When urazoles **17a–c** were treated with Ni_2O_3 in the same manner as described for **3**, colored solutions characteristic of urazole radicals were *not* observed to form even though the starting urazole was consumed as judged by TLC. Upon filtration and concentration of each of these solutions, white solid products were obtained which did not exhibit N–H stretches in the IR spectrum ruling out dimerized products akin to the formation of **11** from **10**. Furthermore, unlike radical **10** for which NMR data could not be obtained due to its paramagnetic nature, the ¹H and ¹³C NMR spectra of solutions of the products isolated from these oxidations were readily obtained. These observations, in addition to the lack of formation of characteristic colors upon dissolution in organic solvents, suggests that for these three systems the tetrazane dimers are considerably more stable than the corresponding urazole radical species (see Scheme 4). While similar tetrazane dimers are known,⁹ to our knowledge this is the first report of urazole radicals that are heavily weighted to the tetrazane dimer side of the equilibrium while in solution. The ¹H NMR spectra for the tetrazane dimer derived from urazole radical **18a** was well behaved but showed unique chemical shifts for all three methyl groups as well as both protons on the

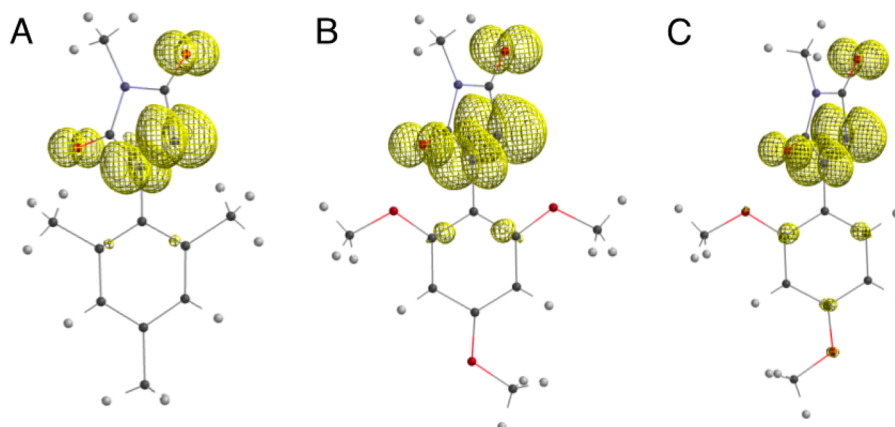


Figure 6. Spin density maps calculated at the UB3LYP/6-31G* level of theory (isovalue = 0.004) for urazole radicals (A) **18a**, (B) **18b**, and (C) **18c**.

aromatic ring (see copies of all of these spectra in the [Supporting Information](#)). One of the methyl groups was significantly upfield (1.48 ppm) of the remaining two (2.23 and 2.24 ppm). Additionally, the ^{13}C NMR spectrum displayed six individual carbon atoms for the aromatic rings in addition to three unique carbon atoms for the benzene methyl groups. The NMR spectra for the tetrazane dimer from **18b** exhibited similar characteristics. The reason for this behavior most likely derives from the crowded structure required for these dimers that heavily restrict free rotation about the C–N bond between the urazole nitrogen atom and the aromatic ring ([Figure 7](#)). A conformation such as

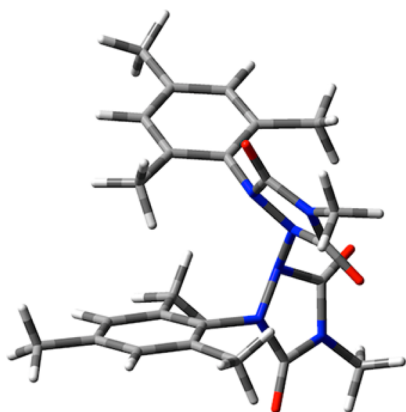


Figure 7. Minimized geometry for the tetrazane dimer derived from urazole radical **18a** at the B3LYP/6-31G* level of theory.

this would account for the single upfield shift of one of the CH_3 groups of the tetrazane dimer of **18a** (and one of the OCH_3 groups from the tetrazane dimer of **18b**), as one group is necessarily suspended within the shielding cone of the aromatic ring of the other urazole unit. Further support for restricted rotation derives from the NMR spectra of **18c**. Having a single *ortho*-substituent on the aromatic ring allows for more rotational freedom in this tetrazane dimer than those of **18a,b**. The ^1H and ^{13}C NMR spectra display complex, broadened signals even though the solutions remain colorless suggesting that the signal broadening derives from restricted rotation and not from the presence of free urazole radicals. Heating the sample to 60°C in the NMR probe sharpened the signals in the ^1H NMR spectrum somewhat (see the [Supporting Information](#)). Further heating resulted in the formation of a dark green colored solution as would be expected from the generation of free urazole radicals via dissociation of the tetrazane dimer. Unfortunately, however, this led to decomposition of the sample so that collecting a suitable ^{13}C NMR spectrum was rendered impossible.

Hence, as to why disubstituted products were observed only from the acid-catalyzed reaction of **1** with anisole, it is most likely that the relative instability of urazole radicals **18a–c** inhibits their formation via reaction of **1** with initially formed urazoles **17a–c** thereby preventing further oxidation to a diazenium species which would be required to form disubstituted products.

CONCLUSION

The mechanism by which disubstituted urazole products **4a,b** were formed from the acid-catalyzed reaction of MeTAD (**1**) with anisole has been elucidated. Rapid hydrogen atom abstraction from initially formed urazole **3** by **1** generates a particularly stable and persistent radical **10**. This was confirmed via UV–vis studies and corroborated by generation of **10** by

independent means (i.e., Ni_2O_3 oxidation of **3**). Oxidation of **10** by either radical cation **12** or **16** generates electrophilic diazenium species **6**. Diazenium **6** could be independently generated via electrochemical as well as chemical (thianthrenium perchlorate) oxidation of **10** and demonstrated to react with electron-rich anisole to form products **4a,b** in a ratio equivalent to that of the MeTAD/TFA/anisole reaction suggesting identical electrophiles are active in both cases. The reluctance of other urazoles (e.g., **17a–c**) to engage in a similar series of reactions leading to disubstituted products has been traced to the apparent instability of the required urazole radicals (**18a–c**).

EXPERIMENTAL SECTION

General Methods. Column chromatography was conducted on silica gel (234–400 mesh) using appropriate mixtures of hexanes and EtOAc as eluent as specified. Thin-layer chromatography was performed on precoated silica gel plates (250 mm) and visualized by ultraviolet light. ^1H and ^{13}C NMR spectra were obtained on a 400 MHz NMR spectrometer. Chemical shifts are reported in units of parts per million downfield from TMS. High-resolution mass spectra (HRMS) were acquired via electron spray ionization on an LTQ-FTMS hybrid mass spectrometer. *N*-Methyl-1,3,5-triazoline-3,5-dione (**2**) was synthesized via oxidation of *N*-methylurazole¹⁰ with N_2O_4 according to the literature¹¹ and sublimed before use. Thianthrenium perchlorate was synthesized according to the literature procedure.⁷ CH_2Cl_2 was dried over 3 \AA molecular sieves prior to use. All other chemicals and solvents were obtained from commercial sources and used without further purification.

Reaction of MeTAD (1**) with Anisole.** To a stirring solution of 0.113 g (1 mmol) of MeTAD (**1**) in 10 mL of dry CH_2Cl_2 was added 0.162 g (1.5 mmol) of anisole followed by 160 μL (2 mmol) of TFA. The solution rapidly turned blood red in color. After stirring overnight, the resulting pale pink solution was diluted with 25 mL of CH_2Cl_2 and washed 1×15 mL of 1 M NaOH. The aqueous phase was backwashed with 1×10 mL of CH_2Cl_2 , and the combined organic layers were dried over Na_2SO_4 , filtered, and concentrated. Column chromatography (50:50 hexanes/EtOAc) afforded 0.145 g (44% yield) of a mixture of compounds 1,2-bis(4-methoxyphenyl)-4-methyl-1,2,4-triazolidine-3,5-dione (**4a**) and 1-(2-methoxyphenyl)-2-(4-methoxyphenyl)-4-methyl-1,2,4-triazolidine-3,5-dione (**4b**) in a 60:40 ratio respectively as a white solid (ratio determined by relative integrations in the ^1H NMR spectrum). The aqueous phase was acidified with conc. HCl and washed with 6×10 mL of CH_2Cl_2 . The combined organic layers were dried over Na_2SO_4 , filtered, and concentrated to afford 12.8 mg (6% yield) of 1-(4-methoxyphenyl)-4-methyl-1,2,4-triazolidine-3,5-dione (**3**) as a white solid. Finally, the acidified aqueous layer was concentrated to a white solid. The solid was washed with 2×20 mL of boiling *n*-propanol followed each time by filtration. The combined washes were concentrated to afford 46 mg (40% yield) of 4-methyl-1,2,4-triazolidine-3,5-dione (**5**) as a white solid. All of the compounds isolated have been fully characterized elsewhere.¹ Note that the yield of compounds **4a/4b** reported in this report (44%) differs from that reported earlier (62%).¹ However, the currently reported value is considered to be reliable.

Dimerization of Urazole Radical **10 To Afford 1-[5-Methoxy-2-(4-methyl-3,5-dioxo-1,2,4-triazolidin-1-yl)phenyl]-2-(4-methoxyphenyl)-4-methyl-1,2,4-triazolidine-3,5-dione (**11**).** To a stirring mixture of 60 mg (0.3 mmol) of urazole **3** in 20 mL of dry CH_2Cl_2 were added 300 mg of Na_2SO_4 followed by 170 mg of Ni_2O_3 . The solution rapidly turned deep blue in color. After stirring for 20 min, the reaction mixture was filtered under N_2 pressure through a fine glass frit into a flask. The solution was deoxygenated with a stream of dry N_2 , sealed, and stored in the dark until the radical color was lost (8 days). The resulting pale green solution was concentrated, and the residue was column chromatographed (100% EtOAc) to afford 18 mg (30% yield) of dimer **11** as a pale yellow film. ^1H NMR (CDCl_3) δ 3.20 (s, 3H), 3.21 (s, 3H), 3.70 (s, 3H), 3.74 (s, 3H), 6.72 (d, $J = 2$ Hz, 1H), 6.88 (d, $J = 9.2$ Hz, 2H), 6.89 (dd, $J = 9.0, 2.9$ Hz, 1H), 7.34 (d, $J = 9.2$ Hz, 2H), 7.36 (d,

$J = 9.0$ Hz, 1H), 8.57 (br s, 1H). ^{13}C NMR (CDCl_3) δ 161.2, 158.5, 155.2, 153.7, 153.4, 152.5, 136.1, 131.4, 127.9, 125.2, 123.9, 115.1, 114.7, 109.3, 55.8, 55.4, 26.1, 25.5. HRMS (ESI) m/z : $[\text{M} + \text{H}]^+$ Calcd for $\text{C}_{20}\text{H}_{21}\text{N}_6\text{O}_6$: 441.1523; Found 441.1516.

Reaction of Radical 10 with Anisole as Catalyzed by TFA. A deep blue solution of radical **10** was generated by stirring 30 mg (0.14 mmol) of urazole **3** with 150 mg of Na_2SO_4 and 85 mg of Ni_2O_3 in 10 mL of CH_2Cl_2 for 20 min followed by filtration through a fine glass frit under N_2 pressure. To this stirring solution were added 150 μL (10 equiv) of anisole followed by 21 μL (2 equiv) of TFA via syringe. The solution decolorized within 3 min time followed by subsequent dilution with 25 mL of CH_2Cl_2 and washing with 1×25 mL of 1 M NaOH. The aqueous phase was backwashed with 1×10 mL of CH_2Cl_2 , and the combined organic layers were dried over Na_2SO_4 , filtered, and concentrated. Column chromatography of the residue (50:50 hexanes/EtOAc) afforded 11 mg (25% yield) of a mixture of **4a** and **4b** in a 60:40 ratio, respectively. The aqueous layer was then acidified with conc. HCl and washed with 6×10 mL of CH_2Cl_2 . The combined organic layers were dried over Na_2SO_4 , filtered, and concentrated to afford 12.5 mg of a mixture of urazole **3** and dimer **11** in 25% and 16% yields, respectively, as determined by relative integrations in the ^1H NMR spectrum.

Reaction of Radical 10 with TFA (in the Absence of Anisole). A deep blue solution of radical **10** was generated by stirring 30 mg (0.14 mmol) of urazole **3** with 150 mg of Na_2SO_4 and 85 mg of Ni_2O_3 in 10 mL of CH_2Cl_2 for 20 min followed by filtration through a fine glass frit under N_2 pressure. To this stirring solution were added 21 μL (2 equiv) of TFA via syringe. The deep blue solution turned pale green over 45 min, which was followed by dilution with 25 mL of CH_2Cl_2 and washing with 1×25 mL of 1 M NaOH. The aqueous phase was backwashed with 1×10 mL of CH_2Cl_2 . The aqueous layer was then acidified with conc. HCl and washed with 6×10 mL of CH_2Cl_2 . The combined organic layers were dried over Na_2SO_4 , filtered, and concentrated to afford 22.8 mg of a mixture of urazole **3** and dimer **11** in 6% and 74% yields, respectively, as determined by relative integrations in the ^1H NMR spectrum.

Reaction of Radical 10 in the Presence of Urazole 3. A deep blue solution of radical **10** was generated by stirring 60 mg (0.27 mmol) of urazole **3** with 300 mg of Na_2SO_4 and 170 mg of Ni_2O_3 in 20 mL of CH_2Cl_2 for 20 min followed by filtration through a fine glass frit under N_2 pressure. To this stirring solution of radical **10** was added 45 mg (0.20 mmol, approximately 1 equiv relative to the generated radical) of urazole **3**. The solution was briefly deoxygenated with N_2 , sealed with a septum, and allowed to stir in the dark until the color of the solution turned a pale green (2 days). The reaction mixture was concentrated to afford a mixture of dimer **11** and unreacted **3** as determined by relative integrations in the ^1H NMR spectrum.

Reaction of Radical 10 with Anisole as Catalyzed by Catalytic Thianthrenium Perchlorate. A deep blue solution of radical **10** was generated by stirring 30 mg (0.14 mmol) of urazole **3** with 150 mg of Na_2SO_4 and 85 mg of Ni_2O_3 in 10 mL of CH_2Cl_2 for 20 min followed by filtration through a fine glass frit under N_2 pressure. To this stirring solution were added 30 μL (2 equiv) of anisole followed by ~ 20 drops of a prepared solution of 37 mg (0.12 mmol) of thianthrenium perchlorate in 6 mL of acetonitrile ($\sim 5\%$ of the ThClO_4 was added as determined by mass difference after removing acetonitrile from the remaining solution). The solution decolorized within 5 min time, at which point it was diluted with 25 mL of CH_2Cl_2 and washed 1×25 mL of 1 M NaOH. The aqueous phase was backwashed with 1×10 mL of CH_2Cl_2 , and the combined organic layers were dried over Na_2SO_4 , filtered, and concentrated. Column chromatography of the residue (50:50 hexanes/EtOAc) afforded 14 mg (32% yield) of a mixture of **4a** and **4b** in a 60:40 ratio, respectively. The aqueous layer was then acidified with conc. HCl and washed with 6×10 mL of CH_2Cl_2 . The combined organic layers were dried over Na_2SO_4 , filtered, and concentrated to afford 16 mg of a mixture of urazole **3** and dimer **11** in 29% and 24% yields, respectively, as determined by relative integrations in the ^1H NMR spectrum.

Generation of Diazonium 6 via Oxidation of Radical 10 by Thianthrenium Perchlorate in the Presence of Anisole and 2,6-Lutidine. A deep blue solution of radical **10** was generated by stirring 30

mg (0.14 mmol) of urazole **3** with 150 mg of Na_2SO_4 and 85 mg of Ni_2O_3 in 10 mL of CH_2Cl_2 for 20 min followed by filtration through a fine glass frit under N_2 pressure. To this stirring solution was added 30 μL (2 equiv) of anisole and 10 μL (1 equiv) of 2,6-lutidine. A solution of 41 mg (1 equiv) of thianthrenium perchlorate in 6 mL of acetonitrile was added dropwise until the blue color of the radical was consumed ($\sim 72\%$ of the ThClO_4 was added as determined by mass difference after removing acetonitrile from the remaining solution). The resulting pale yellow solution was then diluted with 25 mL of CH_2Cl_2 and washed with 1×25 mL of 1 M HCl and 1×25 mL of 1 M NaOH. The aqueous phases were each backwashed with 1×10 mL of CH_2Cl_2 , and the combined organic layers were dried over Na_2SO_4 , filtered, and concentrated. Column chromatography of the residue (50:50 hexanes/EtOAc) afforded 24.3 mg (55% yield based on starting **3**) of a mixture of **4a** and **4b** in a 60:40 ratio, respectively.

Slow Addition of Radical 10 to a Solution of Anisole and TFA. A deep blue solution of radical **10** was generated by stirring 30 mg (0.14 mmol) of urazole **3** with 150 mg of Na_2SO_4 and 85 mg of Ni_2O_3 in 10 mL of CH_2Cl_2 for 20 min followed by filtration through a fine glass frit under N_2 pressure. This solution was taken up in a syringe and added dropwise to a stirring solution of 30 μL (2 equiv) of anisole and 21 μL (2 equiv) of TFA over an hour controlled by a syringe pump. The first part ($\sim 30\%$) of the solution resulted in rapid decolorization of the blue radical color to afford a colorless solution, but as addition continued the color of the solution turned pale green and progressed to an emerald green by the end of the hour. The resulting solution was stirred for an additional 0.5 h without any change in color. It was then diluted with 25 mL of CH_2Cl_2 and washed with 1×25 mL of 1 M NaOH. The aqueous phase was backwashed with 1×10 mL of CH_2Cl_2 , and the combined organic layers were dried over Na_2SO_4 , filtered, and concentrated. Column chromatography of the residue (50:50 hexanes/EtOAc) afforded 16 mg (35% yield) of a mixture of **4a** and **4b** in a 60:40 ratio, respectively. The aqueous layer was then acidified with conc. HCl and washed with 6×10 mL of CH_2Cl_2 . The combined organic layers were dried over Na_2SO_4 , filtered, and concentrated to afford 16 mg of a mixture of urazole **3** and dimer **11** in 29% and 25% yields, respectively, as determined by relative integrations in the ^1H NMR spectrum.

Oxidation of Urazole 17a to 4-Methyl-1-[4-methyl-3,5-dioxo-2-(2,4,6-trimethylphenyl)-1,2,4-triazolidin-1-yl]-2-(2,4,6-trimethylphenyl)-1,2,4-triazolidine-3,5-dione (i.e., Dimer of Radical 18a). To a stirring solution of 32 mg (0.14 mmol) of urazole **17a** in 10 mL dry of CH_2Cl_2 were added 150 mg of Na_2SO_4 followed by 85 mg of Ni_2O_3 . The mixture was stirred for 1 h, filtered through a fine glass frit under N_2 pressure, and concentrated to afford 32 mg (quantitative) of a white solid, mp 160 $^\circ\text{C}$ (decomp). IR (ATR) cm^{-1} 2921, 1689, 1467. ^1H NMR (CDCl_3) δ 1.48 (s, 3H), 2.23 (s, 3H), 2.25 (s, 3H), 3.22 (s, 3H), 6.36 (s, 1H), 6.81 (s, 3H); ^{13}C NMR (CDCl_3) δ 154.2, 149.9, 140.5, 140.2, 137.7, 129.6, 128.8, 127.5, 26.1, 21.2, 18.2, 16.8. HRMS (ESI) m/z : $[\text{M} + \text{H}]^+$ calcd for $\text{C}_{24}\text{H}_{29}\text{N}_6\text{O}_4$: 465.2250; found 465.2245.

Oxidation of Urazole 17b to the 4-Methyl-1-[4-methyl-3,5-dioxo-2-(2,4,6-trimethoxyphenyl)-1,2,4-triazolidin-1-yl]-2-(2,4,6-trimethoxyphenyl)-1,2,4-triazolidine-3,5-dione (i.e., dimer of Radical 18b). To a stirring solution of 38 mg (0.14 mmol) of urazole **17b** in 10 mL of dry CH_2Cl_2 were added 150 mg of Na_2SO_4 followed by 85 mg of Ni_2O_3 . The mixture was stirred for 1 h, filtered through a fine glass frit under N_2 pressure, and concentrated to afford 38 mg (quantitative) of a white solid, mp 179 $^\circ\text{C}$ (decomp). IR (ATR) cm^{-1} 2951, 1732, 1593, 1120. ^1H NMR (CDCl_3) δ 3.10 (s, 3H), 3.64 (s, 3H), 3.78 (s, 3H), 3.80 (s, 3H), 5.94 (d, $J = 2$ Hz, 1H), 6.08 (d, $J = 2$ Hz, 1H); ^{13}C NMR (CDCl_3) δ 162.9, 159.5, 159.3, 154.0, 153.4, 105.9, 91.3, 91.0, 56.4, 56.3, 55.4, 25.8. HRMS (ESI) m/z : $[\text{M} + \text{H}]^+$ calcd for $\text{C}_{24}\text{H}_{29}\text{N}_6\text{O}_{10}$: 561.1945; found 561.1944.

Oxidation of Urazole 17c to 1-(2,4-Dimethoxyphenyl)-2-[2-(2,4-dimethoxyphenyl)-4-methyl-3,5-dioxo-1,2,4-triazolidin-1-yl]-4-methyl-1,2,4-triazolidine-3,5-dione (i.e., Dimer of Radical 18c). To a stirring solution of 34 mg (0.14 mmol) of urazole **17c** in 10 mL of dry CH_2Cl_2 were added 150 mg of Na_2SO_4 followed by 85 mg of Ni_2O_3 . The mixture was stirred for 1 h, filtered through a fine glass frit under N_2 pressure, and concentrated to afford 33 mg (quantitative) of a white solid, mp 188 $^\circ\text{C}$ (decomp). IR (ATR) cm^{-1} 2924, 1730, 1448. ^1H NMR (CDCl_3 , 60 $^\circ\text{C}$) δ 3.10 (brs, 3H), 3.72 (br s, 3H), 3.79 (s, 3H),

6.34 (br s, 2H), 7.00 (br s, 1H). HRMS (ESI) m/z : $[M + H]^+$ calcd for $C_{22}H_{25}N_6O_8$: 501.1734; found 501.1731.

UV-vis Spectroscopic Analysis of Mixtures of MeTAD (1) and Urazoles. A 30 mM stock solution of *N*-methyl-1,2,4-triazoline-3,5-dione (1) was prepared by dissolving 34 mg (0.30 mmol) of freshly sublimed 1 in 10 mL of dry CH_2Cl_2 . To 1 mL of this solution in a cuvette were added 2 mL of fresh CH_2Cl_2 to provide a 10 mM solution, and the UV-vis spectrum was collected.

To analyze for a potential reaction between 1 and urazoles 17a–c, approximately 7–8 mg of urazole were added directly to 3 mL of a 10 mM solution of 1 in a cuvette, the resulting mixture was stirred for 30 min, and the UV-vis spectrum was collected. No new species were observed to form with these urazoles. For urazole 3, 7 mg of compound were added, the mixture was stirred briefly, and spectrum was collected in under 2 min. If the mixture was allowed to sit for longer periods of time, a precipitate formed on the sides of the cuvette (probably the urazole resulting from reduction of MeTAD) that prevented data collection. The spectrum of the resulting radical 10 was obtained by subtracting the UV-vis spectrum of 1 (10 mM) from the spectrum of the mixture (Figure 1).

The UV-vis spectrum of independently prepared radical 10 was collected by stirring 9 mg of urazole 3 with 25 mg of Na_2SO_4 and 25 mg of Ni_2O_3 in 4 mL of CH_2Cl_2 for 30 min followed by filtration through a fine glass frit under N_2 pressure. The resulting 10 mM solution was diluted to 0.5 mM for data collection (Figure 1).

Electrochemical Measurements. High purity anhydrous acetonitrile was used as solvent for all measurements. Deep blue solutions of radical 10 (~4.5 mM) were prepared by stirring 10 mg (4.5×10^{-5} mol) of urazole 3 with 40 mg of Na_2SO_4 and 25 mg of Ni_2O_3 in 10 mL of CH_3CN for 20 min followed by filtration through a fine glass frit under N_2 pressure. Tetrabutylammonium hexafluorophosphate (0.4 g) was then added to make a 0.1 M supporting electrolyte solution. A 15 mL vial was used to contain 10 mL of electrolyte and sealed with a customized Teflon cap holding the three electrodes used. Clean platinum wires were used for both the working and counter electrodes. The reference electrode was a commercially available SCE electrode. The porous glass tip of the reference electrode was rinsed with dry acetonitrile prior to insertion into the cell. Cyclic voltammetry was generally performed at 50 mV/s unless otherwise specified. Voltammetry was collected following the convention in which anodic processes (i.e., oxidation of substrate) are assigned a positive current.

Computations. All geometry minimizations were carried out using the Gaussian 09 suite of software and conducted at the UB3LYP/6-31G* level.¹² Frequency calculations were carried out at the same level of theory to ensure that the geometry represented a true minimum (i.e., no negative frequencies). Spin expectation values $\langle S^2 \rangle$ suggested no appreciable spin contamination for any of the radicals (see Supporting Information). The spin density maps were generated from within Spartan'14 software using the geometries generated by the Gaussian minimizations, also at the UB3LYP/6-31G* level.¹³

■ ASSOCIATED CONTENT

Supporting Information

The Supporting Information is available free of charge on the ACS Publications website at DOI: 10.1021/acs.joc.5b02520.

¹H and ¹³C NMR spectra for all newly characterized compounds. Cartesian coordinates, single-point energies for all computationally minimized structures, and spin expectation values ($\langle S^2 \rangle$) for radical species (PDF)

■ AUTHOR INFORMATION

Corresponding Author

*E-mail: gbretton@berry.edu.

Notes

The authors declare no competing financial interest.

■ ACKNOWLEDGMENTS

This material is based upon work supported by the National Science Foundation under CHE-1125616. G.B. also thanks the Berry College Faculty Development Grant program for support of this research.

■ REFERENCES

- Bretton, G. W. *Tetrahedron Lett.* **2011**, *52*, 733–735.
- (a) Gravel, P. L.; Pirkle, W. H. *J. Am. Chem. Soc.* **1974**, *96*, 3335–3336. (b) Pirkle, W. H.; Gravel, P. L. *J. Org. Chem.* **1977**, *42*, 1367–1369. (c) Pirkle, W. H.; Gravel, P. L. *J. Org. Chem.* **1978**, *43*, 808–815.
- Bausch, M. J.; David, B.; Dobrowolski, P.; Guadalupe-Fasano, C.; Gostowski, R.; Selmarten, D.; Prasad, V.; Vaughn, A.; Wang, L. - H. *J. Org. Chem.* **1991**, *56*, 5643–5651.
- Bard, A. J.; Faulkner, L. R. *Electrochemical Methods, Fundamentals and Applications*, 2nd ed.; John Wiley: New York, 2001; pp 239–242.
- Galabov, B.; Koleva, G.; Schaefer, H. F., III; Schleyer, P. v. R. *J. Org. Chem.* **2010**, *75*, 2813–2819.
- Gstach, H.; Seil, P.; Schantl, J. G.; Gieren, A.; Hubner, T.; Wu, J. *Angew. Chem., Int. Ed. Engl.* **1986**, *25*, 1132–1134.
- Murata, Y.; Shine, H. J. *J. Org. Chem.* **1969**, *34*, 3368–3372.
- (a) Lorans, J.; Hurvois, J. P.; Moinet, C. *Acta Chem. Scand.* **1999**, *53*, 807–813. (b) Varmaghani, F.; Nematollahi, D.; Mallakpour, S. *J. Electrochem. Soc.* **2012**, *159*, F174–F180.
- See, for example (a) Kluge, R.; Omelka, L.; Reinhardt, M.; Schulz, M. *Chem. Ber.* **1992**, *125*, 2075–2079. (b) Barton, D. H. R.; Ozbalik, N.; Vacher, B. *Tetrahedron* **1988**, *44*, 7385–7392. (c) Kealy, T. J. *J. Am. Chem. Soc.* **1962**, *84*, 966–973. (d) Wilmarth, W. K.; Schwartz, N. *J. Am. Chem. Soc.* **1955**, *77*, 4551–4557.
- Bretton, G. W.; Turlington, M. *Tetrahedron Lett.* **2014**, *55*, 4661–4663.
- Mallakpour, S. E. *J. Chem. Educ.* **1992**, *69*, 238–241.
- Frisch, M. J.; Trucks, G. W.; Schlegel, H. B.; Scuseria, G. E.; Robb, M. A.; Cheeseman, J. R.; Scalmani, G.; Barone, V.; Mennucci, B.; Petersson, G. A.; Nakatsuji, H.; Caricato, M.; Li, X.; Hratchian, H. P.; Izmaylov, A. F.; Bloino, J.; Zheng, G.; Sonnenberg, J. L.; Hada, M.; Ehara, M.; Toyota, K.; Fukuda, R.; Hasegawa, J.; Ishida, M.; Nakajima, T.; Honda, Y.; Kitao, O.; Nakai, H.; Vreven, T.; Montgomery, J. A., Jr.; Peralta, J. E.; Ogliaro, F.; Bearpark, M.; Heyd, J. J.; Brothers, E.; Kudin, K. N.; Staroverov, V. N.; Kobayashi, R.; Normand, J.; Raghavachari, K.; Rendell, A.; Burant, J. C.; Iyengar, S. S.; Tomasi, J.; Cossi, M.; Rega, N.; Millam, J. M.; Klene, M.; Knox, J. E.; Cross, J. B.; Bakken, V.; Adamo, C.; Jaramillo, J.; Gomperts, R.; Stratmann, R. E.; Yazyev, O.; Austin, A. J.; Cammi, R.; Pomelli, C.; Ochterski, J. W.; Martin, R. L.; Morokuma, K.; Zakrzewski, V. G.; Voth, G. A.; Salvador, P.; Dannenberg, J. J.; Dapprich, S.; Daniels, A. D.; Farkas, Ö.; Foresman, J. B.; Ortiz, J. V.; Cioslowski, J.; Fox, D. J. *Gaussian 09*, revision D.01; Gaussian, Inc.: Wallingford, CT, 2009.
- Shao, Y.; Molnar, L. F.; Jung, Y.; Kussmann, J.; Ochsenfeld, C.; Brown, S. T.; Gilbert, A. T. B.; Slipchenko, L. V.; Levchenko, S. V.; O'Neill, D. P.; DiStasio, R. A., Jr.; Lochan, R. C.; Wang, T.; Beran, G. J. O.; Besley, N. A.; Herbert, J. M.; Lin, C. Y.; Van Voorhis, T.; Chien, S. H.; Sodt, A.; Steele, R. P.; Rassolov, V. A.; Maslen, P. E.; Korambath, P. P.; Adamson, R. D.; Austin, B.; Baker, J.; Byrd, E. F. C.; Dachsel, H.; Doerksen, R. J.; Dreuw, A.; Dunietz, B. D.; Dutoi, A. D.; Furlani, T. R.; Gwaltney, S. R.; Heyden, A.; Hirata, S.; Hsu, C.-P.; Kedziora, G.; Khalliulin, R. Z.; Klunzinger, P.; Lee, A. M.; Lee, M. S.; Liang, W. Z.; Lotan, I.; Nair, N.; Peters, B.; Proynov, E. I.; Pieniazek, P. A.; Rhee, Y. M.; Ritchie, J.; Rosta, E.; Sherrill, C. D.; Simmonett, A. C.; Subotnik, J. E.; Woodcock, H. L., III; Zhang, W.; Bell, A. T.; Chakraborty, A. K.; Chipman, D. M.; Keil, F. J.; Warshel, A.; Hehre, W. J.; Schaefer, H. F.; Kong, J.; Krylov, A. I.; Gill, P. M. W.; Head-Gordon, M. *Phys. Chem. Chem. Phys.* **2006**, *8*, 3172–3191.